Kaleidoscope

Volume 10 Article 12

June 2012

Geometric Variables Shock-Tunnel Configurations and their Effects on Pressure-Time Waveforms

Chase W. Guengerich

Mark A. Faulhaber
ugresearch@uky.edu

Introduction/Background Information

A shock tunnel is simply a tunnel having either a rectangular or circular cross-sectional area, and is usually constructed of steel. The use of a shock tunnel provides means of rendering parallel results from a large-scale explosion while using a minimized amount of product and space, thus dramatically reducing costs. The University of Kentucky Explosives Research Team (UKERT) has a shock tunnel which was constructed in October 2007. This tunnel is a single rectangular prism chamber; its dimensions are 8 feet wide by 8 feet high by 120 feet long. The current shock tunnel used by UKERT is nearing the end of its useful career and needs to be replaced. The purpose of this study is to determine which tunnel configuration would produce the more accurate results, either a rectangular or circular cross-sectional area. This experiment tests the peak pressure, impulse, and time of arrival for each shot. It is crucial to have uniformity in these components, to assure that the data is not being distorted. Scaling laws were used in this study to calculate the grams of RDX to use for each shot. The standoff distances used in the shock tunnels were calculated from scaled diameters. This is described in full in one of the following sections titled, "Scaling Laws."

Shock Tunnel Application

A shock tunnel does not magnify the amount of energy released from an explosive, rather it focuses the energy. This is similar to a water hose; if the hose is left un-tampered with, the water will flow out. However, if the path of escape is restricted, the water will project further and the water flow becomes more focused. Although the energy within a shock tunnel is confined and focused, there is a still loss in energy due to the shockwave's propagation down the shock tunnel. To study what affect the geometry of a shock tunnel has on the waveform dynamics, two shock tunnels of equal cross-sectional area and volume are being used. This is described fully in the "Shock Tunnel Testing" section.

Scaling Laws

The characteristics of the blast wave generated in an explosion depend both on the explosive energy release and on the nature of the medium through which the blast propagates. These characteristics are readily defined quantitatively for any particular explosion. Applying the scaling principle to explosions, two (different) explosions can be expected to give identical blast wave intensities at distances which are proportional to the cube root of the respective energy release (Kinney, 1962). In this experiment, scaling laws were used to determine the scaled distance, as well as the weight (g) of RDX to use for a shot. The scaled distance was calculated using Hopkinson cubed root and square root scaling equations. These two equations are shown below, labeled as Equation 1.1 A and Equation 1.1 B. The weights (g) of RDX used per shot were calculated through the scaled distance equation 1.2 A, and through the linear scaling equation 1.2 B.

Equation 1.1 A

$$D_S = \left(\frac{D}{\sqrt[3]{W}} \right)$$

Equation 1.1 B

$$D_S = \left(\frac{D}{\sqrt{W}} \right)$$

Equation 1.2 A

$$W = \left(\frac{D}{D_S} \right)^2$$

Equation 1.2 B

$$\frac{W_{Large}}{Area_{Large}} = \frac{W_{Small}}{Area_{Small}}$$

€

Shock Tunnel Testing

Testing was done in two separate shock tunnels of different geometric configurations. The two shock tunnels used in the experiment possessed the same cross-sectional area and volume. The first tunnel had a rectangular cross-section of 10.6 inches by 10.6 inches and was 20 feet long. The second tunnel had a circular cross-section with a diameter of 12 inches and was 20 feet long; both tunnels having a cross-sectional area of 113 square inches. The purpose of this test was to analyze the data collected from both shock tunnels in conjunction with one another to understand how the geometry of a shock tunnel affects the peak pressure, impulse, and time of arrival for each shot.

Shock Tunnel Experimental Design

Within the two shock tunnels, five Flush Mount Reflected Pressure Piezoelectric Transducers (Reflected Pressure Sensors) were mounted onto a steel plate located at one end of the tunnel. The same sensor plate was used to measure the waveform dynamics in both the circular and rectangular shock tunnels. The arrangement of these Reflected Pressure Sensors were set in a cross pattern; three sensors across the center with one sensor above and below the middle sensor. Figure 1 is a representation of the cross-section of both shock tunnels.

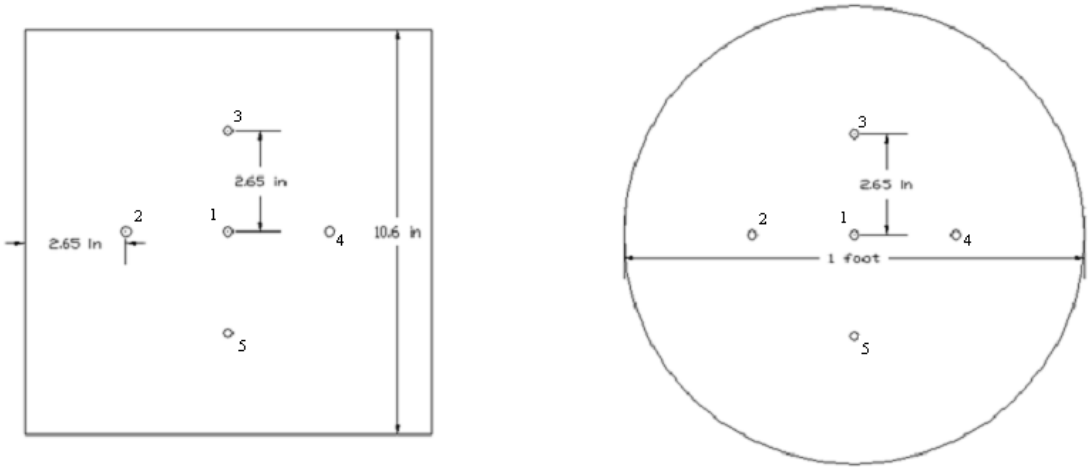

Figure 1

To study the effects that varying shock tunnel configurations have on waveform dynamics, three charge weights of RDX were placed at three separate stand-off distances. The charge weights used were 3 grams, 6.2 grams and 11 grams. These weights were determined by using the scaling laws mentioned earlier. Each charge weight was shot at stand-off distances of 1.5 feet, 3 feet, 4.4 feet, and 6 feet. These weights and stand-off distances were used in both the rectangular and circular cross-section shock tunnel. The data collected from the Reflected Pressure Sensors in both the rectangular and circular cross section shock tunnels was analyzed and is summarized in the following "Data Analysis" section.

Data Analysis

This study originally called for a total of 18 shots, which consisted of 2 different weights (3 grams, 11 grams) at three offset distances (1.5 feet, 3 feet, 6 feet). These different scenarios were going to be preformed 3 times for uniformity and consistency. Officially, there were a total of 30 shots, with 4 different weights, 3 offset distances, and only a limited number of repeated shots.

To better determine the characteristics of our waveforms inside the shock tunnels, we needed to compare them to actual data from a large shock tunnel. To do this, we scaled our weights down from data we had. After scaling and shooting the corresponding weights and standoff distances, we collected our data. Later,

when analyzing the collected data to compare with the large shock tunnel's data, we realized that the scaled weights and standoff distances were calculated incorrectly. Because this calculation was done incorrectly we were unable to compare our results between the shock tunnels. Due to this error, we rerouted our experiment plan, and tested to compare waveform dynamics between only the circular and square shock tunnel.

The data from the experiments were then filtered into acceptable and unacceptable data. The final accepted data used for calculations is shown here in Table 1.

		Square	Circular
Weight	Distance	Number of successful shots	Number of successful Shots
3	1.5	1	1
11	1.5	1	1
3	3	1	1
11	3	1	1
6.2	4.4	1	1
3	6	2	2
11	6	1	1
Total per shock tunnel		8	8
Total per study		16	

Table 1

Once the data was deemed acceptable, the average pressure for each shot was calculated and tabulated below in Table 3. The average pressures were then plotted and are shown below in Plot 1.

Average Pressure (psi)		
Test	**Rectangular Shock Tunnel**	**Circular Shock Tunnel**
3 g at 1.5 ft	**181.4**	**268.8**
11 g at 1.5 ft	**648.7**	**342.4**
3 g at 3 ft	**114.1**	**90.4**
11 g at 3 ft	**290.5**	**397.9**
6.2 g at 4.4 ft	**137.1**	**141.5**
3 g at 6 ft	**48.4**	**71.7**
3 g at 6 ft	**48.8**	**73.7**
11 g at 6 ft	**141.5**	**168.9**

Table 3

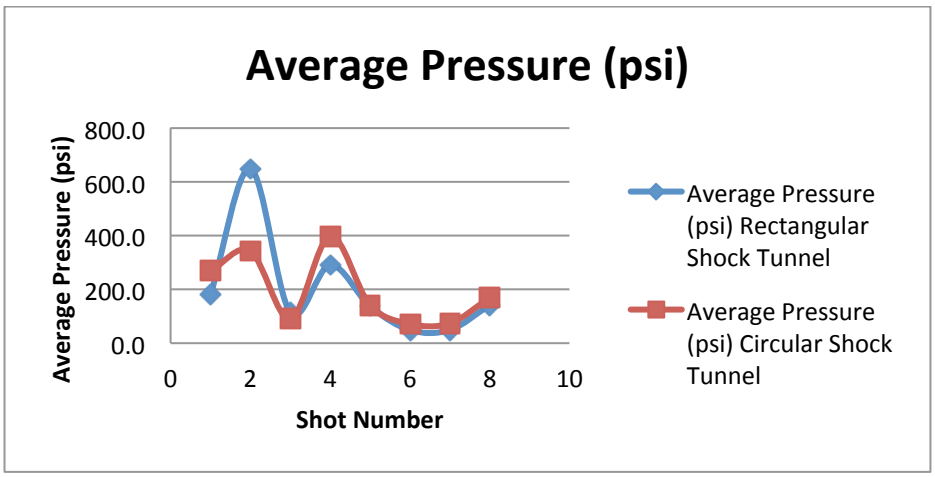

Plot 1

It is seen here that there exists no pattern, uniformity, or consistency in the average pressure in relation to the geometric configuration of a shock tunnel. The average pressures between both shock tunnels tend to follow the same path and are fairly symmetric. However, the square shock tunnel read a higher psi for only two shots, versus the circular shock tunnel which read a higher psi for the remaining six shots. This data is not clear enough to predict that the pressure behavior between both shock tunnel configurations is equal.

In considering the shockwave produced when a charge detonates, we know that it rapidly expands from the center out in a spherical shape. Because the geometric shape of a charge's detonation and the circular tunnel are the same, it could be hypothesized that a circular shock tunnel could concentrate a waveform as it propagates down the tunnel and in turn direct the pressure, producing higher peak pressures.

The square shock tunnel, however, has edges and corners which produced areas that would normally not be consumed by a circular shape. Because a shockwave is circular the waves could be refracting off these corners, and distorting the shock front, which may lead to lower average pressures.

Secondly, we calculated the data to retrieve the impulse. The average impulse was calculated for both shock tunnels and tabulated below in Table 4. The data was then plotted and is shown in Plot 2.

Average Impulse (psi-ms)		
Test	**Rectangular Shock Tunnel**	**Circular Shock Tunnel**
3 g at 1.5 ft	**86.1**	**94.0**
11 g at 1.5 ft	**213.4**	**184.8**
3 g at 3 ft	**80.0**	**89.8**
11 g at 3 ft	**211.8**	**223.5**
6.2 g at 4.4 ft	**170.7**	**166.8**
3 g at 6 ft	**87.2**	**105.9**
3 g at 6 ft	**93.4**	**94.5**
11 g at 6 ft	**245.2**	**179.5**

Table 4

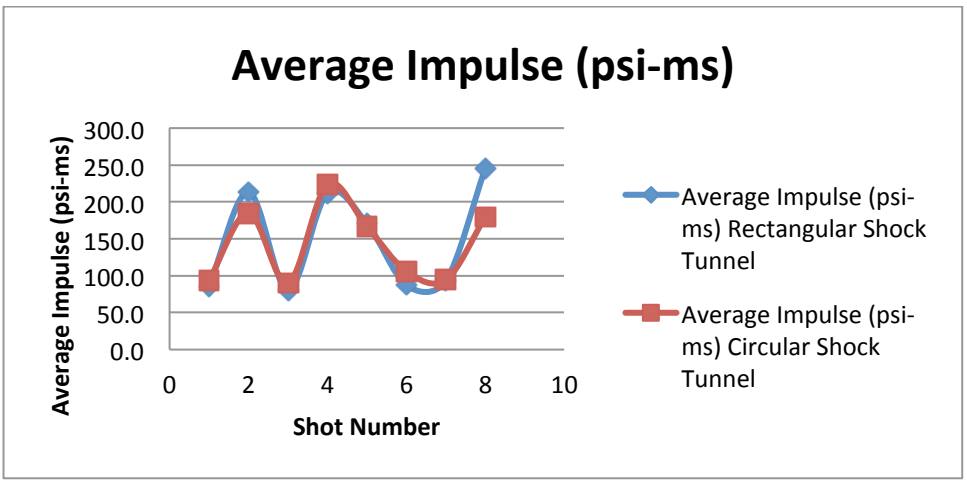

Plot 2

The impulse values for the circular and square shock tunnels were fairly precise. This data is repetitive enough to deduce that regardless of geometric configuration of a shock tunnel, the relation between pressure and time is equal. Plot 2 only reiterates the independency of impulse with relation to geometric configuration.

Thirdly, the time of arrival for each reflected pressure sensor was calculated and then averaged. After, the standard deviation for the time of arrival for each shot and both shock tunnels was calculated and tabulated below in Table 5. These values were then plotted and are shown below in Plot 3.

Time of Arrival				
	Rectangular Shock Tunnel		Circular Shock Tunnel	
Test	Average TOA (ms)	Standard Deviation	Average TOA (ms)	Standard Deviation
3 g at 1.5 ft	0.0045	0.0038	0.2888	0.0025
11 g at 1.5 ft	0.0655	0.0048	0.0074	0.0086
3 g at 3 ft	0.6512	0.0078	0.2508	0.0092
11 g at 3 ft	0.5773	0.0069	0.0080	0.0054
6.2 g at 4.4 ft	0.4058	0.0000	0.0080	0.0054
3 g at 6 ft	2.3596	0.0024	2.2995	0.0053
3 g at 6 ft	2.5238	0.0035	0.9686	0.0014
11 g at 6 ft	0.0048	0.0016	0.0074	0.0048

Table 5

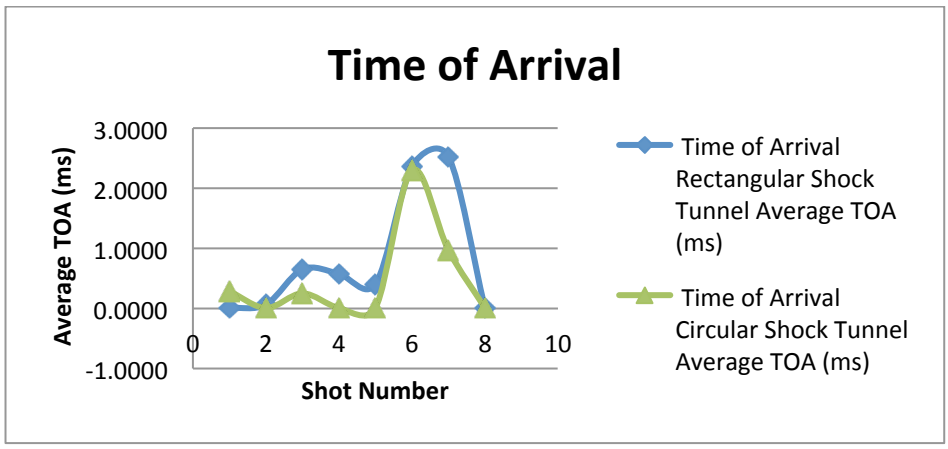

Plot 3

This data does not prove that the time of arrival for both shock tunnels are similar nor does it suggest that one shock tunnel configuration produces a more uniform or planar shock front. The results that were calculated show that, the time of arrival for both geometric configurations tends to follow the same shape as far as the graph is concerned. This means they tend to have comparable behaviors when focusing on time.

Conclusions

The average impulse between the circular and that of the square shock tunnels possess similar characteristics. When the values are plotted, the graph of eacg shock tunnel behaves similarly. This proves that regardless of geometric configuration, the average impulse will be nearly the same in value.

The average pressure when compared between the shock tunnel configurations is scattered. The retrieved and calculated data is not stable enough to deduce an educated conclusion. However, the behavior of the graphs shows that the pressure with relation to charge size and standoff distances tends to follow similar trends.

The time of arrival between each shock tunnel follows the same phenomena as the impulse and pressure. Though the graphs are similar, it cannot be concluded as to whether one shock tunnel creates a more planar shock front than the other.

This experiment needs to be revisited and further explored in order to produce results or conclusions that can be used in real- world application. To gather more useful information from this study, we need to compare results from the new, smaller shock tunnels, to the previous large shock tunnel. If comparable data is gathered from the large shock tunnel, than we can investigate hether one shock tunnel's configuration mimics the behavior of the large shock tunnel better than the other.

Appendix A

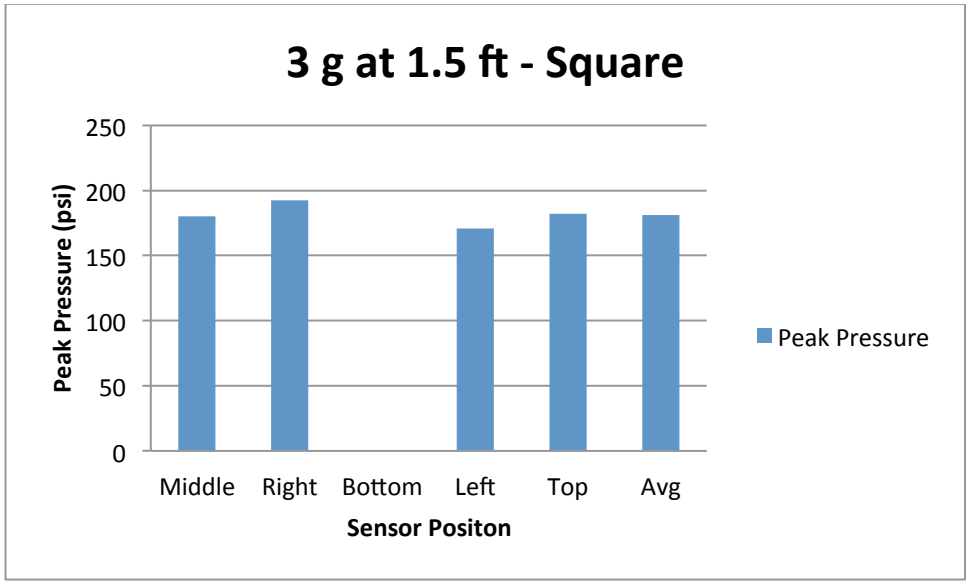
3 g at 1.5 ft - Square
Peak Pressure (psi)
250
200
150
100
50
0
Middle
Right
Bottom
Left
Top
Avg
Sensor Positon
Peak Pressure

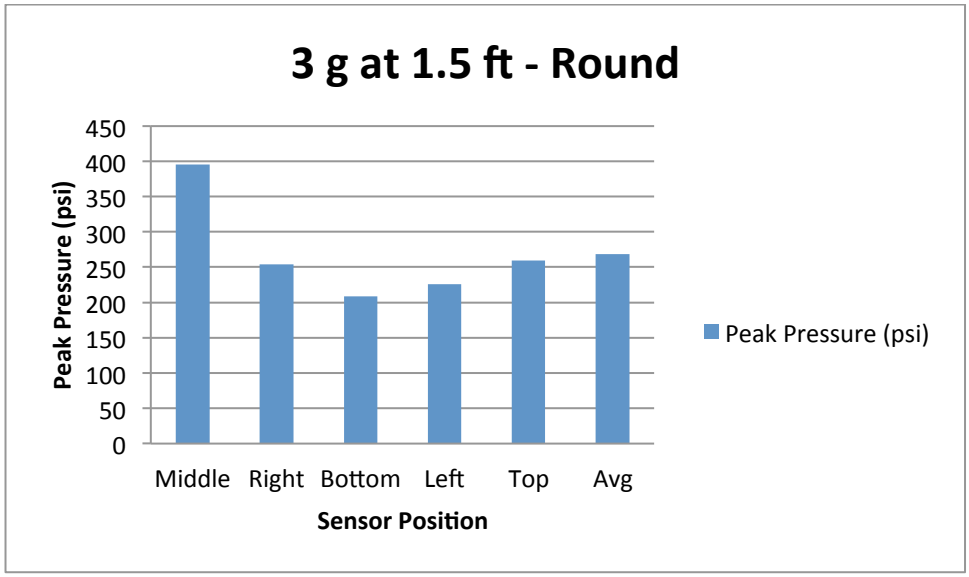
3 g at 1.5 ft - Round
Peak Pressure (psi)
450
400
350
300
250
200
150
100
50
0
Middle
Right
Bottom
Left
Top
Avg
Sensor Position
Peak Pressure (psi)

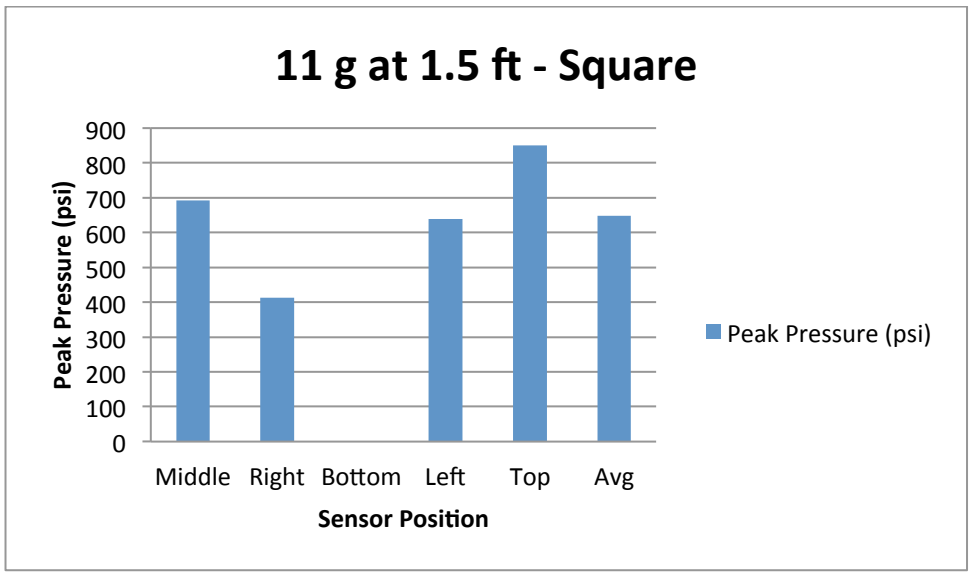
11 g at 1.5 ft - Square
Peak Pressure (psi)
900
800
700
600
500
400
300
200
100
0
Middle
Right
Bottom
Left
Top
Avg
Sensor Position
Peak Pressure (psi)

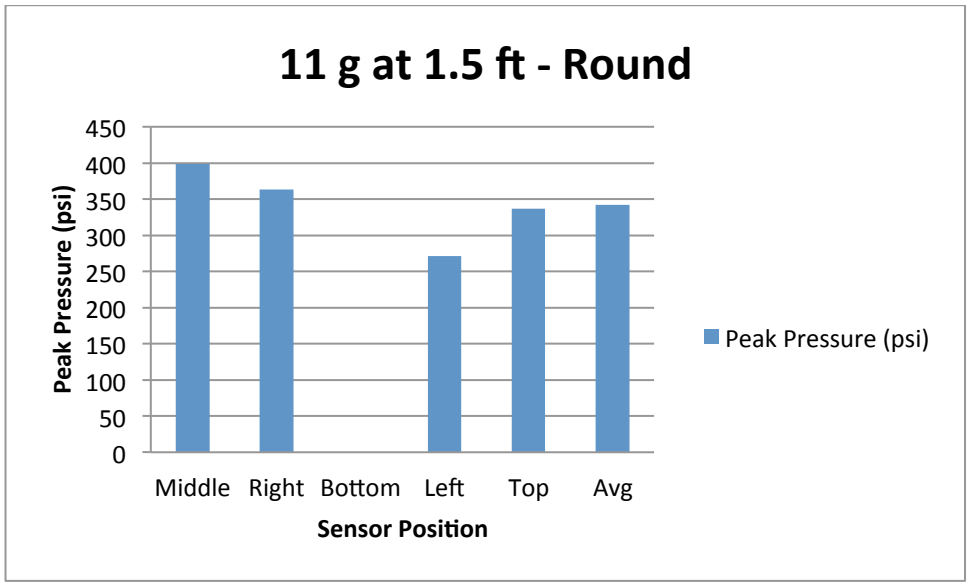
11 g at 1.5 ft - Round
Peak Pressure (psi)
450
400
350
300
250
200
150
100
50
0
Middle
Right
Bottom
Left
Top
Avg
Sensor Position
Peak Pressure (psi)

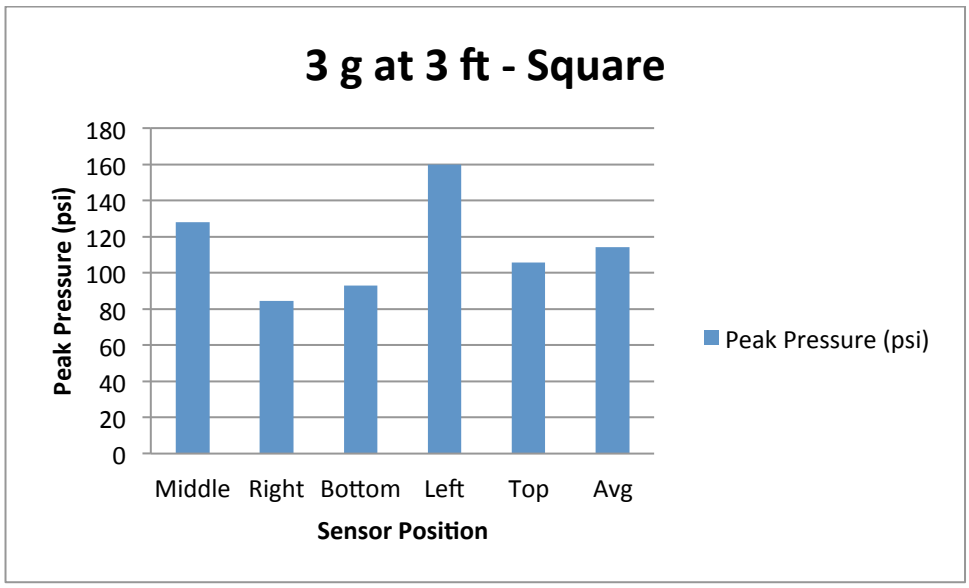
3 g at 3 ft - Square
Peak Pressure (psi)
180
160
140
120
100
80
60
40
20
0
Middle
Right
Bottom
Left
Top
Avg
Sensor Position
Peak Pressure (psi)

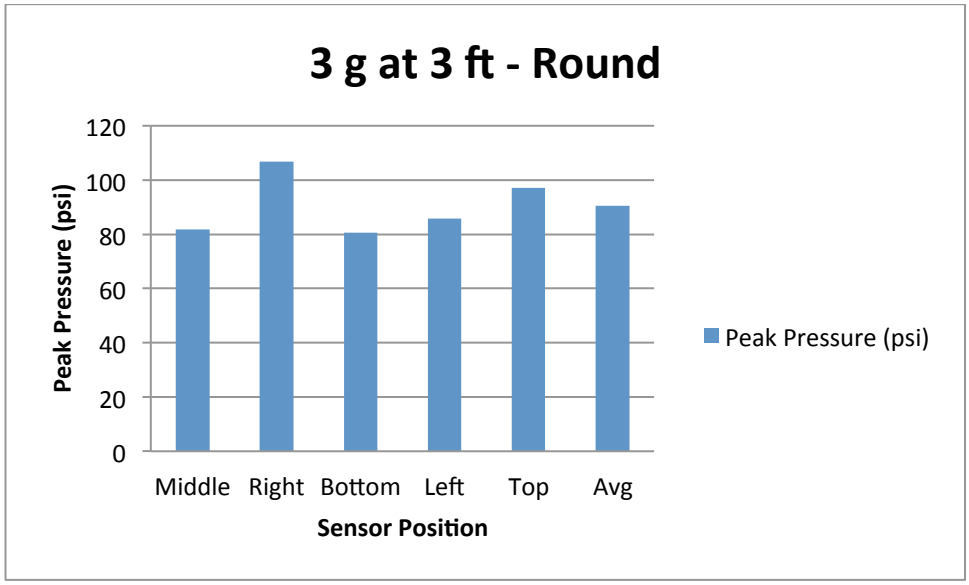
3 g at 3 ft - Round
Peak Pressure (psi)
120
100
80
60
40
20
0
Middle
Right
Bottom
Left
Top
Avg
Sensor Position
Peak Pressure (psi)

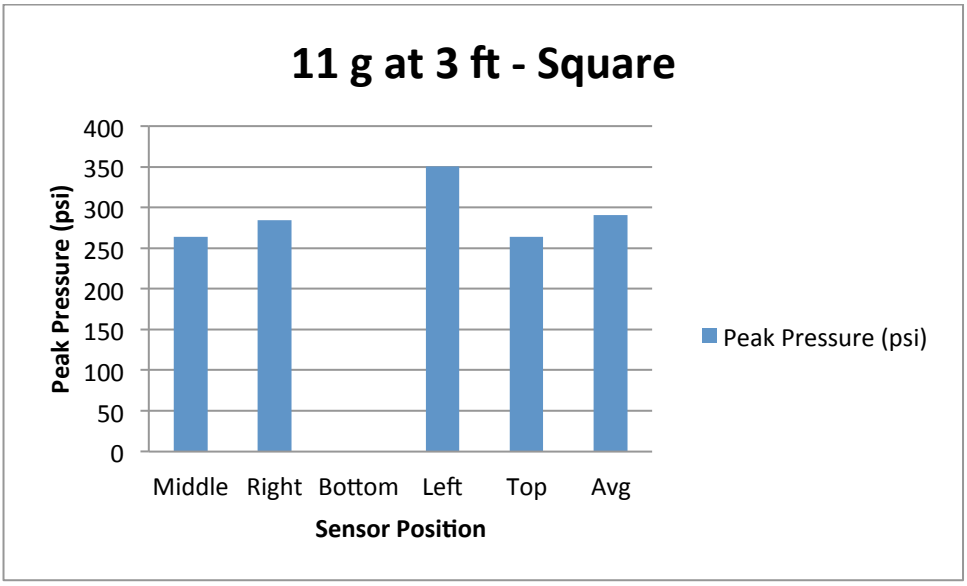
11 g at 3 ft - Square
Peak Pressure (psi)
400
350
300
250
200
150
100
50
0
Middle
Right
Bottom
Left
Top
Avg
Sensor Position
Peak Pressure (psi)

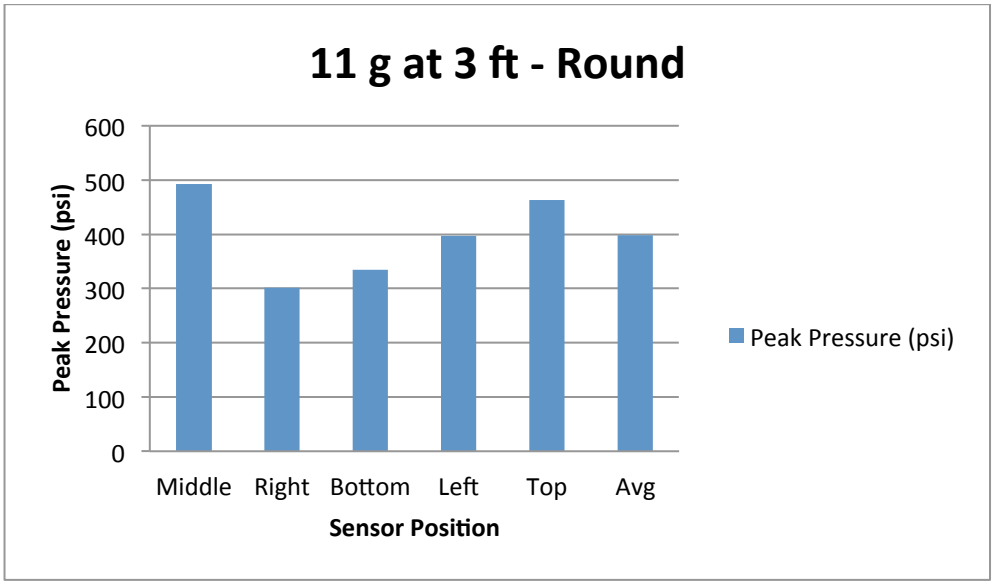
11 g at 3 ft - Round
Peak Pressure (psi)
600
500
400
300
200
100
0
Middle
Right
Bottom
Left
Top
Avg
Sensor Position
Peak Pressure (psi)

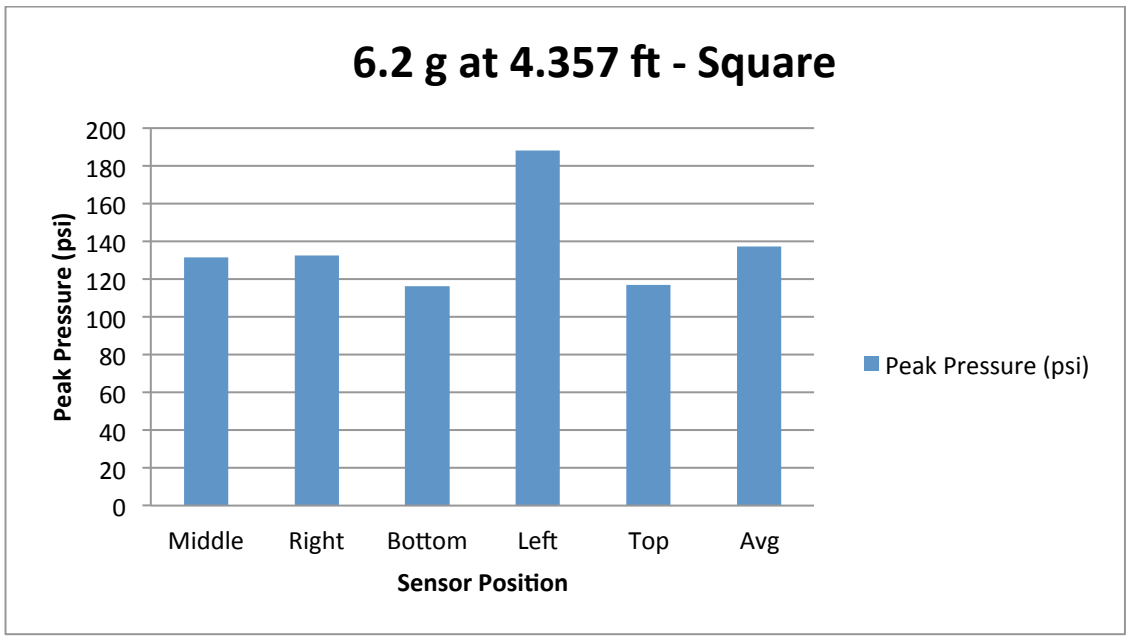
6.2 g at 4.357 ft - Square
Peak Pressure (psi)
200
180
160
140
120
100
80
60
40
20
0
Middle
Right
Bottom
Left
Top
Avg
Sensor Position
Peak Pressure (psi)

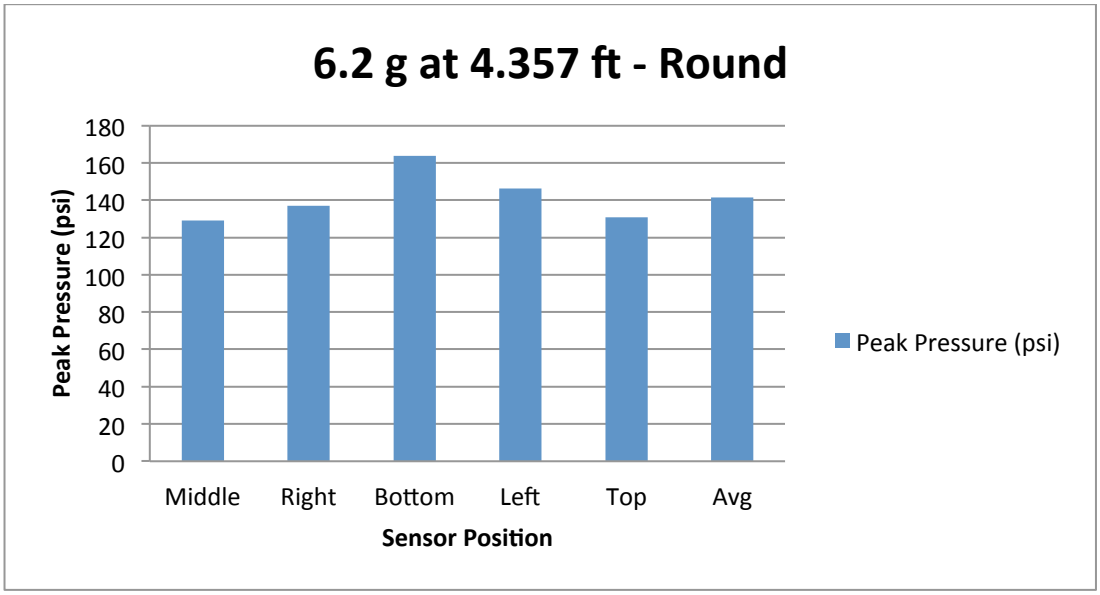
6.2 g at 4.357 ft - Round
Peak Pressure (psi)
180
160
140
120
100
80
60
40
20
0
Middle
Right
Bottom
Left
Top
Avg
Sensor Position
Peak Pressure (psi)

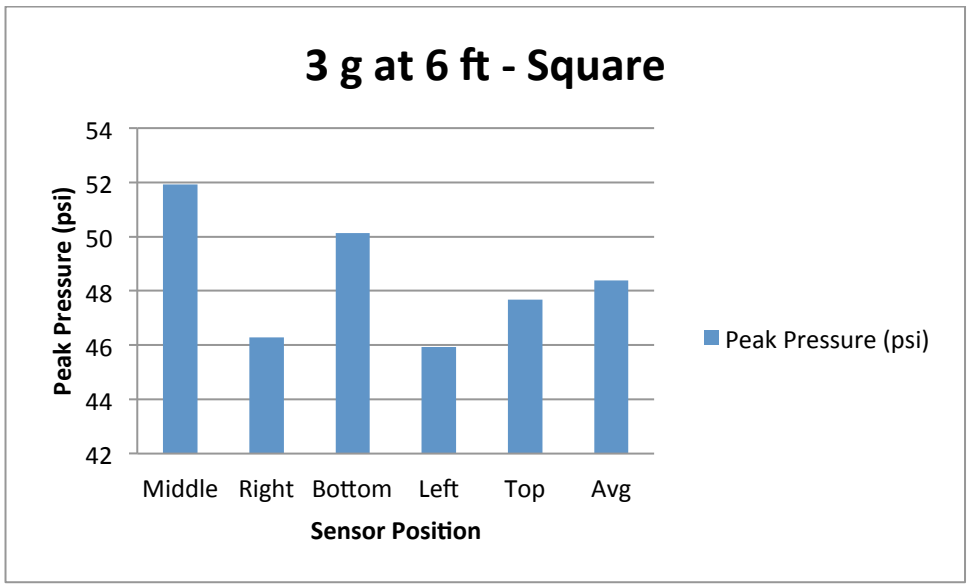
3 g at 6 ft - Square
Peak Pressure (psi)
54
52
50
48
46
44
42
Middle
Right
Bottom
Left
Top
Avg
Sensor Position
Peak Pressure (psi)

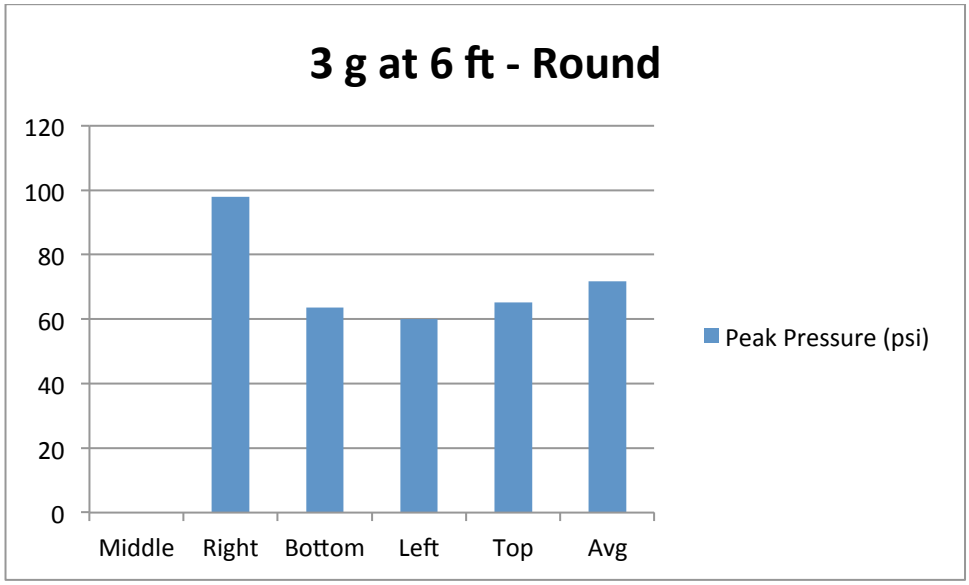
3 g at 6 ft - Round
120
100
80
60
40
20
0
Middle
Right
Bottom
Left
Top
Avg
Peak Pressure (psi)

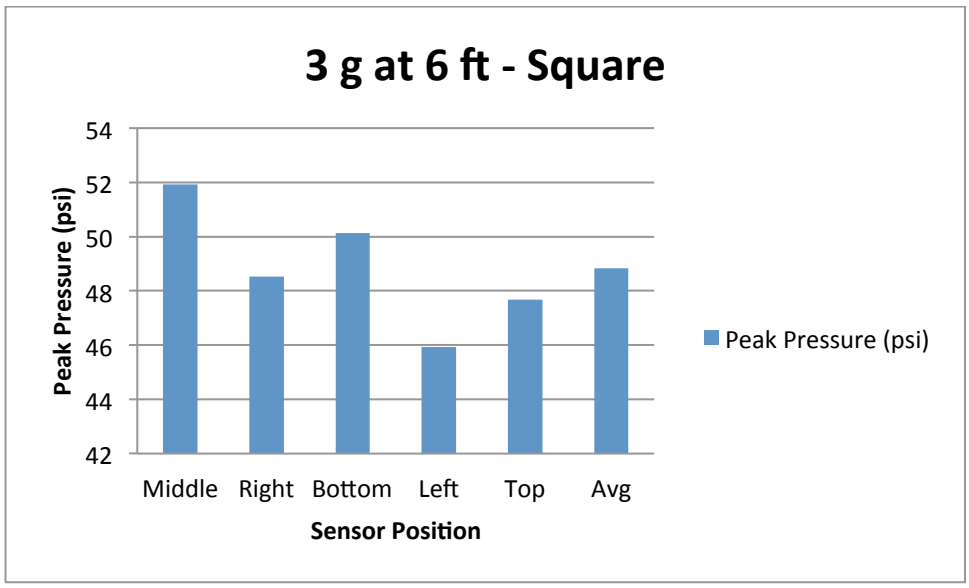
3 g at 6 ft - Square
Peak Pressure (psi)
54
52
50
48
46
44
42
Middle
Right
Bottom
Left
Top
Avg
Sensor Position
Peak Pressure (psi)

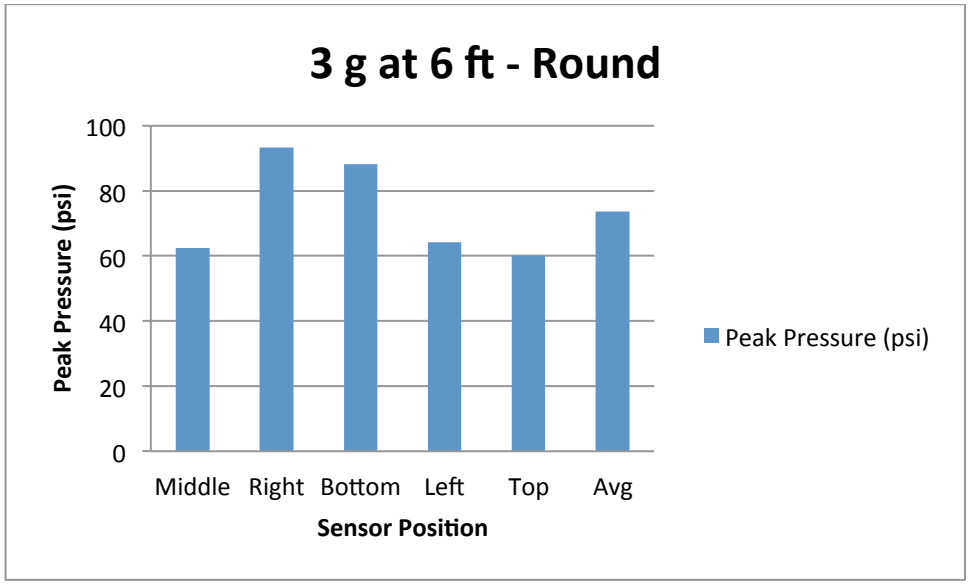
3 g at 6 ft - Round
Peak Pressure (psi)
100
80
60
40
20
0
Middle
Right
Bottom
Left
Top
Avg
Sensor Position
Peak Pressure (psi)

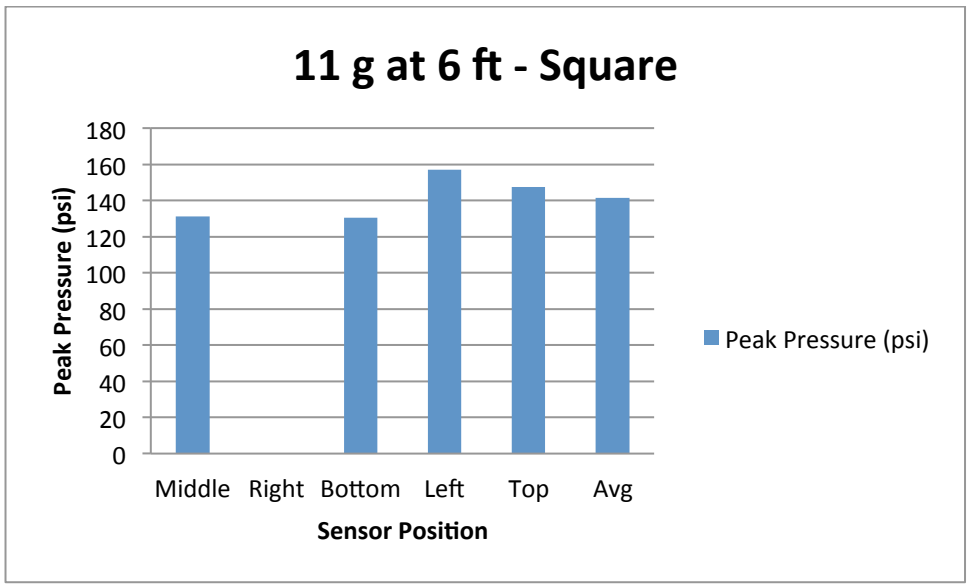
11 g at 6 ft - Square
Peak Pressure (psi)
180
160
140
120
100
80
60
40
20
0
Middle
Right
Bottom
Left
Top
Avg
Sensor Position
Peak Pressure (psi)

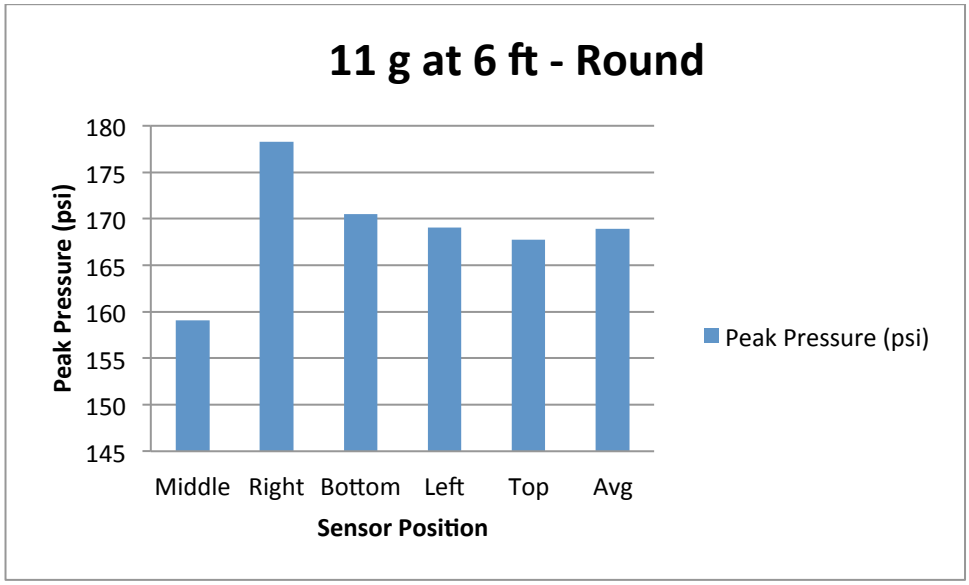
11 g at 6 ft - Round
Peak Pressure (psi)
180
175
170
165
160
155
150
145
Middle
Right
Bottom
Left
Top
Avg
Sensor Position
Peak Pressure (psi)

Appendix B

Day 1 Rectangular					Day 1 Circular			
Shot	Description	Pressure	Impluse		Shot	Description	Pressure	Impluse
1	3 g at 6 ft	48.4	87.2		1			
2	3 g at 6 ft	48.8	93.4		2			
3	11 g at 6 ft	No Results	No Results		3			
4	No Test	No Test	No test		4	No Test	No test	No test
5	11 g at 6 ft	No Results	No Results		5			
6					6	3 g at 6 ft	71.7	105.9
7					7	3 g at 6 ft	73.7	94.5
8					8	11 g at 6 ft	179.5	173.3
9					9	11 g at 6 ft	168.9	179.5
10	11 g at 6 ft	141.5	245.2		10			
11	11 g at 6 ft	148.0	178.8		11			
Day 2 Rectangular					Day 2 Circular			
Shot	Description	Pressure	Impluse		Shot	Description	Pressure	Impluse
1	3 g at 3 ft	114.1	80.0		1			
2	3 g at 1.5 ft	181.4	86.1		2			
3	11 g at 3 ft	290.5	211.8		3			
4	11 g at 1.5 ft	648.7	213.4		4			
5					5	3 g at 3 ft	2783.3	462.7
6					6	3 g at 1.5 ft	268.8	94.0
7					7	11 g at 3 ft	397.9	223.5
8					8	11 g at 1.5 ft	1743.7	207.8
9					9	6.2 g at 4.4 ft	141.5	166.8
10	6.2 g at 4.4 ft	137.1	170.7		10			
11	.77 g at 4.4 ft	1318.6	1786.3		11			
12					12	.77 g at 4.4 ft	9434.5	10945.7
Day 3 Rectangular					Day 3 Circular			
Shot	Description	Pressure	Impluse		Shot	Description	Pressure	Impluse
1					1	3 g at 1.5 ft	44.8	109.4
2					2	11 g at 1.5 ft	342.4	184.8
3					3	3 g at 3 ft	90.4	89.8
4					4	.77 g at 4.4 ft	30.2	22.6
5	3g at 1.5 ft	No Data	No Data		5			
6	3 g at 1.5 ft	No Data	No Data		6			
7	11 g at 1.5 ft	260.2	139.1		7			
8	3 g at 3 ft	506.2	348.5		8			
9	.77 g at 4.4 ft	54.2	36.2		9			
10	3g at 1.5 ft	134.9	96.1		10			